Autonomic Neuroscience: Basic and Clinical 186 (2014) 62–68

Contents lists available at ScienceDirect

Autonomic Neuroscience: Basic and Clinical

journal homepage: www.elsevier.com/locate/autneu

Acute effects of arterial baroreflex on sympathetic nerve activity and plasma norepinephrine concentration

Toru Kawada [a,*], Tsuyoshi Akiyama [b], Shuji Shimizu [a], Yusuke Sata [a,c], Michael J. Turner [a], Mikiyasu Shirai [b], Masaru Sugimachi [a,c]

[a] Department of Cardiovascular Dynamics, National Cerebral and Cardiovascular Center, Osaka 565-8565, Japan
[b] Department of Cardiac Physiology, National Cerebral and Cardiovascular Center, Osaka 565-8565, Japan
[c] Department of Artificial Organ Medicine, Faculty of Medicine, Osaka University Graduate School of Medicine, Osaka 565-0871, Japan

ARTICLE INFO

Article history:
Received 16 July 2014
Received in revised form 6 October 2014
Accepted 15 October 2014

Keywords:
Carotid sinus baroreflex
Open-loop analysis
Arterial pressure
Neuronal uptake blockade

ABSTRACT

Arterial pressure (AP) elevates as a logarithmic function of exogenously administered dose of norepinephrine (NE). In contrast, AP is nearly linearly correlated with efferent sympathetic nerve activity (SNA) during acute baroreflex intervention. The present study aimed at quantifying the relationship between SNA and plasma NE concentration during acute baroreflex intervention. Carotid sinus regions were isolated from systemic circulation in five Wistar Kyoto rats, and carotid sinus pressure was changed among 60, 100, 120, 140, and 180 mm Hg every 2 min. Arterial blood (0.2 ml) was obtained at each pressure level for plasma NE measurement. Maximum AP and minimum AP were 153.34 ± 6.28 and 67.31 ± 4.92 mm Hg, respectively, in response to pressure perturbation. Plasma NE correlated linearly with SNA for individual animal data (slope: 0.957 ± 0.090 $pg \cdot ml^{-1} \cdot \%^{-1}$, intercept: 46.57 ± 7.22 pg/ml, r^2: ranged from 0.923 to 0.992) and also for group averaged data (NE = 0.956 × SNA + 47.97, $r^2 = 0.982$). Blockade of neuronal NE uptake by intravenous desipramine (1 mg/kg) administration increased the slope (2.966 ± 0.686 $pg \cdot ml^{-1} \cdot \%^{-1}$, $P < 0.05$) and the intercept (168.73 ± 28.53 pg/ml, $P < 0.01$) of the plasma NE–SNA relationship. These results indicate that the relationship between SNA and plasma NE concentration was nearly linear within the normal physiological range of acute baroreflex control of AP. While plasma NE concentration can reflect changes in SNA, it may also overestimate the sympathetic outflow from the central nervous system when neuronal NE uptake is impaired systemically.

1. Introduction

The arterial baroreflex is an important negative feedback system that stabilizes arterial pressure (AP) during daily activities. The sympathetic nervous system plays a dominant role in the acute baroreflex control of AP. Studies using an isolated carotid sinus baroreceptor preparation have revealed that AP correlates almost linearly with efferent sympathetic nerve activity (SNA) when examined by a staircase-wise pressure input protocol in anesthetized rats (Kawada et al., 2009, 2010, 2011, 2014; Yamamoto et al., 2013). Norepinephrine (NE) is a neurotransmitter released into the synaptic cleft at sympathetic nerve endings. Although a large portion of NE is removed from the synaptic cleft by neuronal and extraneuronal NE uptake mechanisms (Eisenhofer, 2001; Nicholls, 1994; Shimizu et al., 2010), a fraction of NE is diffused into the bloodstream and can be measured as plasma NE. While it is conceivable that plasma NE concentration reflects the level of SNA, an exact relationship between SNA and plasma NE concentration during an acute baroreflex intervention remains unknown. In contrast to the almost linear AP response to SNA observed in acute baroreflex studies, AP elevates with the logarithm of exogenously administered dose of NE (Yamaguchi and Kopin, 1980) or the logarithm of plasma NE concentration during electrical spinal cord stimulation in pithed rats (Yamaguchi and Kopin, 1979). On the other hand, administration of calcium antagonists exhibits good inverse correlations between AP and the logarithm of plasma NE concentration (Imai et al., 1994). If plasma NE concentration is logarithmically associated with AP, the linearity between SNA and AP would indicate that plasma NE concentration exponentially increases as a function of SNA. To test this hypothesis, the present study aimed to quantify the relationship between SNA and plasma NE concentration during acute baroreflex intervention. In addition, the effect of neuronal NE uptake blockade on the relationship between SNA and plasma NE concentration was explored to quantitatively understand the importance of neuronal NE uptake in the determination of plasma NE concentration.

2. Materials and methods

Animal care was provided in strict accordance with the *Guiding Principles for the Care and Use of Animals in the Field of Physiological*

* Corresponding author at: Department of Cardiovascular Dynamics, National Cerebral and Cardiovascular Center, 5-7-1 Fujishirodai, Suita, Osaka 565-8565, Japan. Tel.: +81 6 6833 5012x2427; fax: +81 6 6835 5403.
E-mail address: torukawa@ncvc.go.jp (T. Kawada).

http://dx.doi.org/10.1016/j.autneu.2014.10.016
1566-0702/

Sciences, approved by the Physiological Society of Japan. All protocols were reviewed and approved by the Animal Subject Committee of National Cerebral and Cardiovascular Center.

Male Wistar Kyoto rats (330–380 g) were anesthetized with an intraperitoneal injection (2 ml/kg) of a mixture of urethane (250 mg/ml) and α-chloralose (40 mg/ml), and mechanically ventilated with oxygen-supplied room air. Anesthesia was maintained by continuous intravenous infusion of a diluted solution of the above anesthetic mixture. An arterial catheter was inserted into the right femoral artery to measure AP. Another arterial catheter was inserted into the left common carotid artery to obtain arterial blood samples. Body temperature of the animal was maintained at approximately 38 °C using a heating pad and a lamp.

A postganglionic branch of the splanchnic sympathetic nerve was exposed retroperitoneally through a left flank incision for the measurement of splanchnic SNA (spSNA). A pair of stainless steel wire electrodes (Bioflex wire, AS633, Cooner Wire, CA, USA) was attached to the nerve, and were secured with silicone glue (Kwik-Sil, World Precision Instruments, FL, USA). A preamplified nerve signal was band-pass filtered at 150 — 1000 Hz, and then full-wave rectified and low-pass filtered at a cut-off frequency of 30 Hz using analog circuits. A ganglionic blocker hexamethonium bromide (60 mg/kg) was given intravenously at the end of the experiment to confirm the disappearance of spSNA and to measure the noise level (Kawada et al., 2010).

The aortic depressor nerves and the vagus nerves were sectioned bilaterally to minimize reflex effects from the aortic arch and cardiopulmonary regions. Bilateral carotid sinuses were isolated from system circulation according to previously reported procedures (Sato et al., 1999; Shoukas et al., 1991). The isolated carotid sinuses were filled with warmed Ringer's solution through catheters inserted into the common carotid arteries. Carotid sinus pressure (CSP) was controlled using a servo-controlled piston pump. Heparin sodium (100 U/kg) was given intravenously to prevent blood coagulation. After completing the above surgery, a stabilization period of at least 60 min was allowed before data acquisition.

2.1. Protocol 1 ($n = 5$)

To determine the time course of plasma NE response to carotid sinus baroreflex, CSP was first set at 100 mm Hg. After AP reached a steady state, CSP was increased to 140 mm Hg. Arterial blood (0.2 ml) was sampled at 80, 50, and 20 s before the step change in CSP and at 30, 60, 90, 120, 150, and 180 s after the step change in CSP. Each blood sampling procedure took approximately 15 s. To avoid contamination of the blood within a catheter, an initial 0.2-ml blood was withdrawn into a temporary syringe that had been filled with 0.2-ml saline, the following 0.2-ml blood was taken as a sample, and then the initial blood, admixed with saline, was returned into the artery. The blood samples were immediately iced to 4 °C. After the end of the protocol, the blood samples were centrifuged and plasma NE concentrations were measured using a high-performance liquid chromatography system (Eicom, Kyoto, Japan) after an alumina adsorption procedure.

2.2. Protocol 2 ($n = 5$)

To determine the relationship between spSNA and plasma NE over a wide input pressure range of the carotid sinus baroreflex, CSP was first decreased to 60 mm Hg for 4 min. CSP was then increased to 100, 120, 140, and 180 mm Hg in a staircase manner. Each step was maintained for 120 s. Based on the time course of plasma NE response obtained in *Protocol 1*, arterial blood (0.2 ml) was sampled at 100 s in each CSP step. The blood sampling procedure took approximately 15 s, as described in *Protocol 1*, and had finished before the next CSP change occurring at 120 s. After obtaining control data, a neuronal uptake blocker desipramine (1 mg/kg) was administered intravenously. Twelve minutes later, the staircase-wise CSP input was repeated and corresponding data were obtained.

2.3. Protocol 3 ($n = 5$)

As a supplemental protocol, the effect of exogenous NE administration on AP was examined. Carotid sinuses were not isolated, and the aortic depressor nerves and vagus nerves were untouched in this group. Instead, ganglionic transmission was blocked by intravenous bolus injection of hexamethonium bromide (60 mg/kg). After 30-min stabilization, the AP response to intravenous continuous administration of NE was examined. The dose of NE was changed every 15 min in an increasing order at 0.05, 0.1, 0.5, 1, 5, 10, 50, 100, 500, and 1000 $\mu g \cdot kg^{-1} \cdot h^{-1}$.

2.4. Data analysis

CSP, spSNA, and AP were recorded at 1000 Hz using a 16-bit analog-to-digital converter. In *Protocol 1*, mean spSNA recorded during CSP of 100 mm Hg was assigned to 100%, and mean spSNA measured after the ganglionic blockade was assigned to 0% in each animal. For plasma NE data, baseline NE concentration was determined from an average of three data points before the step input in each animal. In addition to the absolute NE concentration, the decrease in plasma NE concentration from the baseline value was expressed as a percentage relative to the decrease observed at the nadir (90 s after the step input). In *Protocol 2*, mean spSNA and AP were obtained by averaging spSNA and AP values from 90 to 100 s, just before the arterial blood sampling, at each CSP level. The mean spSNA corresponding to 60-mmHg CSP was assigned to 100%, and mean spSNA measured after the ganglionic blockade was assigned to 0% in each animal. In *Protocol 3*, the AP value corresponding to each NE dose was derived from an average during the last 1 min of the 15-min administration period.

2.5. Statistical analysis

All data are presented as mean and SE values. In *Protocol 1*, plasma NE concentrations at 30, 60, 90, 120, 150, and 180 s after the step input were compared using one-way repeated-measures analysis of variance (ANOVA). In *Protocol 2*, slope and intercept values were determined in each animal by linear regression, and the parameters were compared before and after the desipramine administration using a paired-t test. Differences were considered significant when $P < 0.05$ (Glantz, 2002). In *Protocol 3*, the relationship between exogenously administered dose of NE and AP was examined using a semilog plot (a linear ordinate versus a logarithmic abscissa) and linear scatter plots.

3. Results

Time series of CSP, AP, and spSNA obtained in *Protocol 1*, and corresponding plasma NE concentrations are shown in Fig. 1. CSP and AP are presented as 10-Hz resampled signals, and spSNA is presented as a 2-s moving averaged signal. Before the step increase in CSP, there were transient AP drops caused by arterial blood sampling for the measurement of plasma NE concentration. After CSP was increased, AP showed a sustained reduction. While spSNA was stable before the step input, it ceased at the onset of the step input. Thereafter, spSNA gradually recovered to approximately 35% of the baseline level after 210 s. The baseline plasma NE concentration was approximately 120 pg/ml. After CSP was increased, plasma NE concentration decreased to approximately 80 pg/ml. While there were no statistically significant differences in plasma NE concentration from 30 to 180 s, a slight nadir was observed at 90 s. If decreases from baseline are expressed as percentages relative to the decrease observed at the nadir, percent decreases were 67.1 ± 8.8% at 30 s, 82.9 ± 4.1% at 60 s, and 100% at 90 s. Thereafter, percent

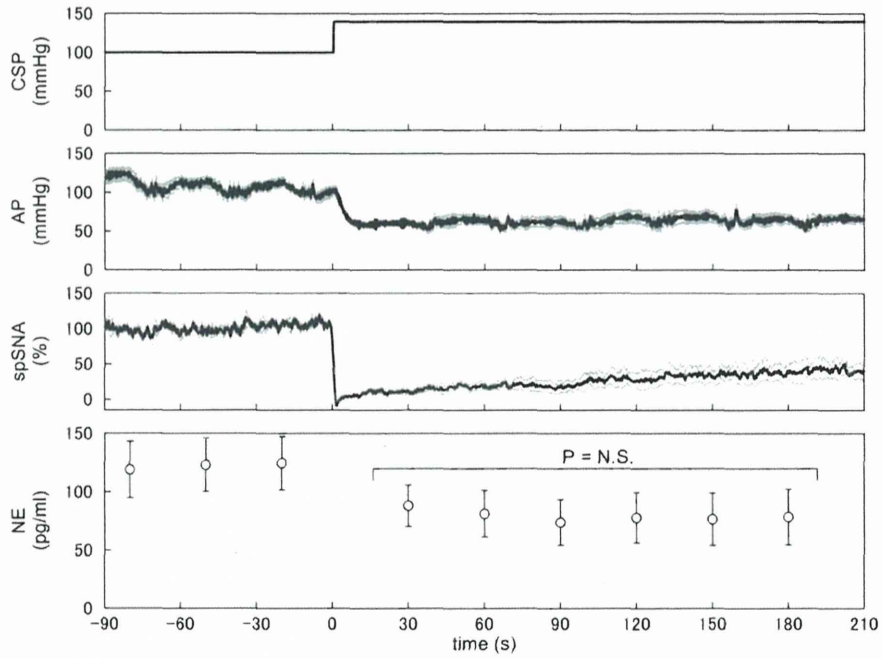

Fig. 1. Time series of carotid sinus pressure (CSP), arterial pressure (AP), and splanchnic sympathetic nerve activity (spSNA), and corresponding plasma norepinephrine (NE) concentration obtained in *Protocol 1*. A step increase in CSP decreased AP and spSNA. Plasma NE concentration decreased in response to the step increase in CSP and did not differ significantly from 30 to 180 s after the step input. Data are mean and SE values.

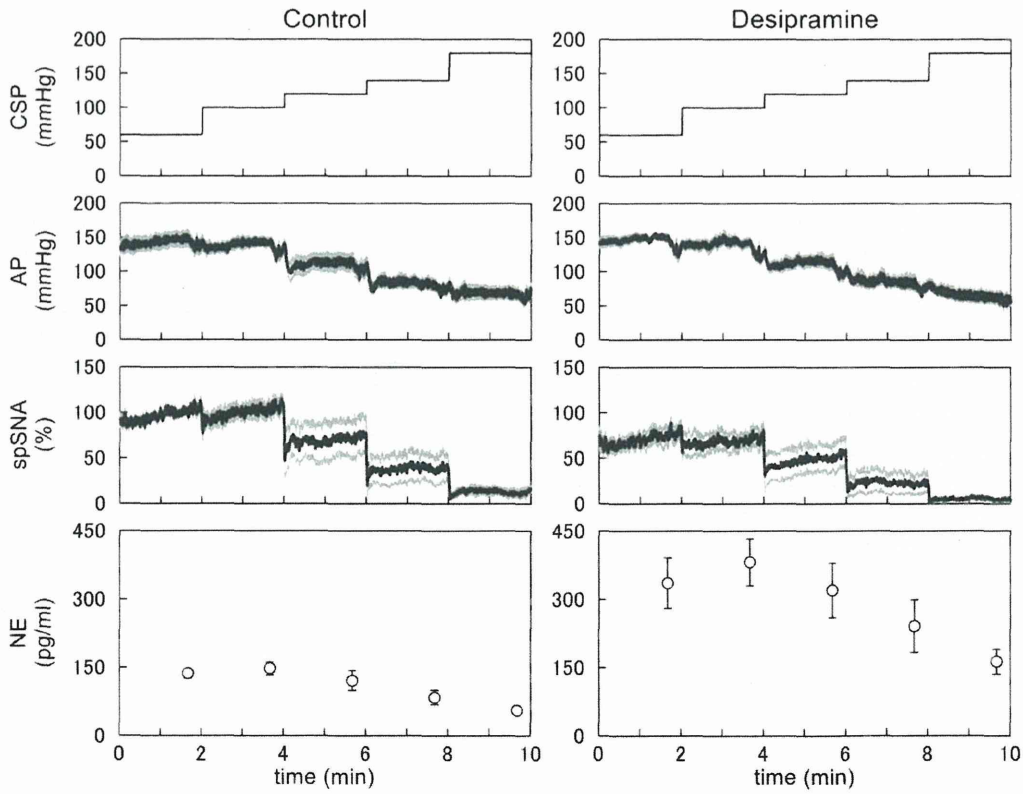

Fig. 2. Time series of arterial pressure (AP) and splanchnic sympathetic nerve activity (spSNA) in response to a staircase-wise increase in carotid sinus pressure (CSP) obtained in *Protocol 2*. Plasma norepinephrine (NE) concentration was decreased as CSP was increased to 120 mm Hg and above. Intravenous administration of desipramine (1 mg/ml) decreased the maximum spSNA but did not change the AP response significantly. Desipramine significantly increased plasma NE concentration compared with the control condition at each corresponding CSP level. Data are mean and SE values.

decreases were relatively stable (92.8 ± 4.5% at 120 s, 93.9 ± 10.8% at 150 s, and 90.4 ± 13.7% at 180 s).

The time series of CSP, AP, and spSNA obtained in *Protocol 2*, and corresponding plasma NE concentrations are shown in Fig. 2. CSP and AP are presented as 10-Hz resampled signals, and spSNA is presented as a 2-s moving averaged signal. An increase in CSP decreased AP and spSNA both under the control condition and after the intravenous administration of desipramine. An increase in CSP from 60 to 100 mm Hg did not decrease plasma NE concentration. Further increases in CSP to 120, 140, and 180 mm Hg decreased plasma NE concentration. Desipramine suppressed the maximum spSNA but did not decrease AP significantly compared with the control condition. Desipramine significantly increased plasma NE concentration compared with the control condition at each CSP level.

In *Protocol 2*, plasma NE concentration was nearly linearly correlated with spSNA for individual animal data with the coefficient of determination (r^2) ranging from 0.923 to 0.992 (Fig. 3A) and also for the group-averaged data with r^2 of 0.982 (Fig. 3G) under the control condition. After desipramine, the data points became convex in two animals (Fig. 3D, "a" and "d") and plasma NE concentrations at high spSNA were greatly dispersed in three animals (Fig. 3D, "b", "d", and "e"). After desipramine, r^2 ranged from 0.791 to 0.940 for individual data (Fig. 3D) and was 0.912 for the group-averaged data (Fig. 3G). On average, desipramine tripled the slope of the regression line (from 0.957 ± 0.090 to 2.966 ± 0.686 pg ml^{-1} $\%^{-1}$, $P < 0.05$) and increased the intercept (from 46.57 ± 7.22 to 168.73 ± 28.53 pg/ml, $P < 0.01$) compared with the control condition (Fig. 3G).

AP was nearly linearly correlated with spSNA for individual animal data with r^2 ranging from 0.855 to 0.991 (Fig. 3B) and also for group-averaged data with r^2 of 0.985 (Fig. 3H) under the control condition. After desipramine, AP was nearly linearly correlated with spSNA for individual data with r^2 ranging from 0.892 to 0.975 (Fig. 3E) and also for group-averaged data with r^2 of 0.997 (Fig. 3H). Desipramine increased the slope of AP versus spSNA (from 0.878 ± 0.082 to 1.212 ± 0.100 mm Hg/%, $P < 0.01$) but did not change the intercept (from 54.16 ± 7.64 to 59.64 ± 6.18%, $P = 0.37$) compared with the control condition (Fig. 3H).

The minimum spSNA was 11.36 ± 4.37% and the maximum spSNA was 106.94 ± 6.02% under the control condition. Note that the maximum spSNA occurred at the CSP level higher than 60 mm Hg in two

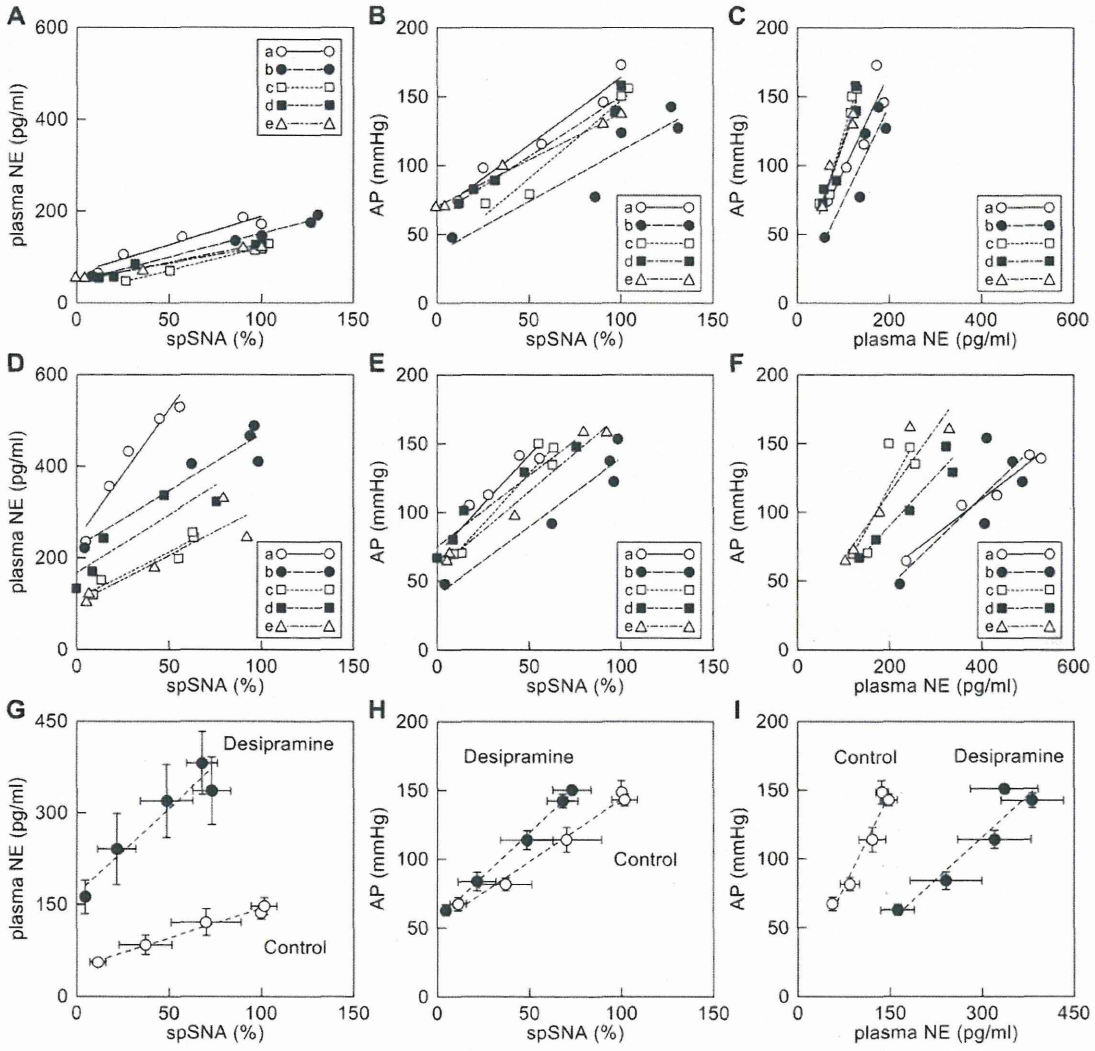

Fig. 3. Relationships between splanchnic sympathetic nerve activity (spSNA) and plasma norepinephrine (NE) concentration (A), spSNA and arterial pressure (AP) (B), and plasma NE concentration and AP (C) under the control condition. Relationships between spSNA and plasma NE concentration (D), spSNA and AP (E), and plasma NE concentration and AP (F) after the intravenous administration of desipramine. In panels A–F, different symbols and regression lines indicate data from different animals. Group-averaged relationships between spSNA and plasma NE concentration (G), spSNA and AP (H), and plasma NE concentration and AP (I) before (open circles) and after (filled circles) intravenous administration of desipramine. In panels G, H, and I, data points indicate mean and SE values, and dotted lines are linear regression lines on averaged data points.

animals, and hence exceeded 100%. Desipramine did not affect the minimum spSNA (4.58 ± 1.50%, P = 0.16) but decreased the maximum spSNA (77.00 ± 8.16%, P = 0.01) compared with the control condition. The minimum AP was 67.31 ± 4.92 mm Hg, the maximum AP was 153.34 ± 6.28 mm Hg, and the range of AP response (i.e., the maximum AP minus the minimum AP) was 86.04 ± 5.43 mm Hg under the control condition. Desipramine decreased the minimum AP (62.74 ± 3.86 mm Hg, P < 0.05) but did not affect the maximum AP (151.16 ± 3.29 mm Hg, P = 0.83) or the range of AP response (88.42 ± 5.67 mm Hg, P = 0.80) compared with the control condition.

AP was nearly linearly correlated with plasma NE concentration for individual animal data with r^2 ranging from 0.817 to 0.965 (Fig. 3C) and also for group-averaged data with r^2 of 0.943 (Fig. 3I) under the control condition. Data points at high AP were greatly dispersed after desipramine, resulting in r^2 ranging from 0.661 to 0.968 for individual data (Fig. 3F) and 0.889 for group-averaged data (Fig. 3I). Desipramine halved the slope of the regression line (from 0.896 ± 0.085 to 0.403 ± 0.061 mm Hg·pg^{-1}·ml, P < 0.001) and tended to decrease the intercept (16.47 ± 3.76 to 4.71 ± 7.03 mm Hg, P = 0.066) compared with the control condition (Fig. 3I).

In *Protocol 3*, AP was linearly correlated with the logarithm of the exogenously administered dose of NE (Fig. 4A). The solid line represents linear regression of AP versus the logarithm of the dose of NE. When linear scales were used, the relationship between the dose of NE and AP did not approximate a straight line even when the range of exogenous NE was limited up to 10 (Fig. 4B) or 100 μg·kg^{-1}·h^{-1} (Fig. 4C). In Fig. 4B and C, the solid curve represents the regression, AP = a × log$_{10}$(NE) + b, determined from the data points up to 1000 μg·kg^{-1}·h^{-1} of NE. The dotted curve also represents the regression but determined from the data points up to 10 (Fig. 4B) or 100 μg·kg^{-1}·h^{-1} (Fig. 4C) of NE. In Fig. 4B and C, the baseline AP after ganglionic blockade was depicted as a filled circle at NE = 0.

4. Discussion

4.1. Relationship between spSNA and plasma NE concentration

As mentioned in the Introduction section, AP changes almost linearly with the amplitude of multifiber spSNA during acute baroreflex intervention (Fig. 3H). In contrast, AP increases with the logarithm of exogenously administered dose of NE (Fig. 4A), and plots of AP versus the dose of NE cannot be linear even when the NE range was limited to lower doses (Fig. 4B and C). Yamaguchi and Kopin (1979) demonstrated that AP increases as a function of the logarithm of plasma NE concentration during electrical spinal cord stimulation in pithed rats. While these results suggest a possible exponential increase of plasma NE concentration as a function of SNA, the present results demonstrated nearly linear relationship between spSNA and plasma NE concentration during acute baroreflex intervention under the control condition (Fig. 3G). The relationship between plasma NE concentration and AP was also almost linear under the control condition (Fig. 3I). Although the maximum sympathetic activation attained by baroreceptor unloading alone might be lower than that attained by direct electrical stimulation of the spinal cord (Yamaguchi and Kopin, 1979), the maximum AP reached 150 mm Hg in *Protocol 2* (Fig. 3I). Therefore, it is likely that the relationship between plasma NE concentration and AP is more linear than commonly thought when examined within the physiological range of baroreflex-mediated AP control. On the other hand, when renal SNA is enhanced by passive muscle stretch on top of the baroreceptor unloading, the AP response becomes saturated, rendering the AP–renal SNA relationship convex curvilinear (Yamamoto et al., 2005). If such data points of excess sympathetic activation are included, AP may be more linearly correlated with the logarithm of SNA and hence the logarithm of plasma NE concentration.

Plasma NE concentrations measured under the control condition (Fig. 3) were lower than those observed during electrical spinal cord stimulation in pithed rats in the absence of anesthesia when compared at the same degree of AP elevation (Yamaguchi and Kopin, 1979). While the maximum AP seemed maintained, anesthesia might have suppressed a sympathetic tone and reduced plasma NE concentration in the present study. Another possible explanation is that the leakage of NE from the sympathetic nerve terminals into the circulation might have been smaller during the baroreflex-mediated sympathetic intervention compared with the sympathetic activation by spinal cord stimulation. Coordinated sympathetic activation among different neural districts is important for the AP control (Guyenet, 2006). While the pithed preparation is useful for investigating sympathetic cardiovascular regulations (Yamaguchi and Kopin, 1979, 1980), stimulation from the spinal cord eliminates the coordinated sympathetic activation. In contrast, because the baroreflex-mediated sympathetic intervention maintains the integrity of the sympathetic pathway from the vasomotor center to the effector organs, the sympathetic nervous system might have operated more efficiently to increase AP. While the stimulation patterns alone (constant, irregular, or burst) do not affect NE overflow or vasoconstriction significantly (Kahan et al., 1988), intermittent and irregular bursting diamond-wave pattern is more effective in reproducing renal functional alterations than continuous square wave pattern (DiBona and Sawin, 1999). Further studies are clearly required to compare the effectiveness of native sympathetic discharge versus electrical stimulation-induced sympathetic activation in the control of AP.

Despite a significant advancement of SNA recording technique in rats (Stocker and Muntzel, 2013), the quantification of chronic changes

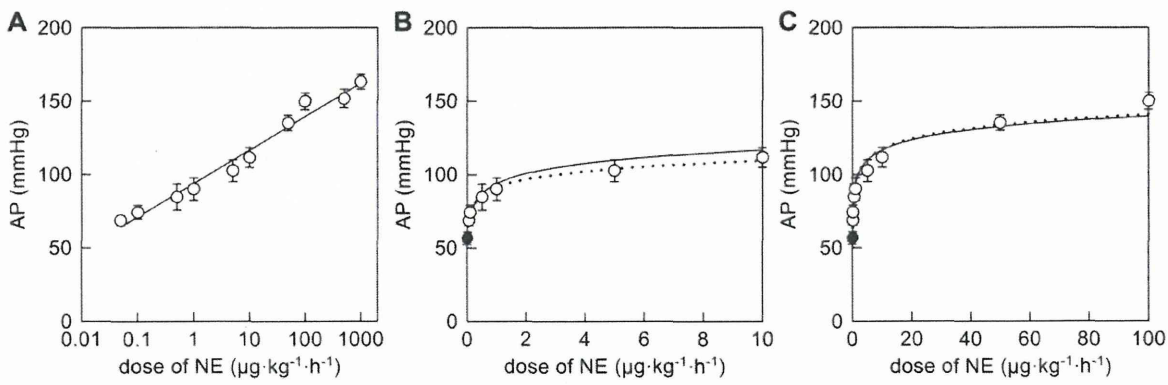

Fig. 4. Relationship between exogenously administered dose of norepinephrine (NE) and steady-state arterial pressure (AP) response shown as a semilog plot (a linear ordinate versus a logarithmic abscissa) (A) and linear scaled scatter plots (B and C). The linear plots include the baseline AP after the ganglionic blockade at NE = 0. The solid line in panel A indicates a linear regression line for AP versus the logarithm of NE. The solid curves in panels B and C indicate the regression, AP = a × log$_{10}$(NE) + b, determined using all data points up to 1000 μg kg^{-1} h^{-1} of NE. The dotted curve indicates the same regression but determined using data points up to 10 (B) and 100 (C) μg kg^{-1} h^{-1} of NE. Data are mean and SE values.

in SNA over long periods (e.g., weeks) is still challenging due to potential time-dependent decline in the amplitude of SNA. The present study demonstrated a nearly linear relationship between plasma NE and spSNA during acute baroreflex intervention (Fig. 3G). If such relationship between SNA and plasma NE is consistent over longer periods, plasma NE levels could be used as a surrogate for SNA. To determine whether plasma NE levels can be a surrogate for SNA in chronic experimental settings may be one of the future directions of the study.

4.2. Effects of neuronal uptake blockade on spSNA and plasma NE concentration

In *Protocol 2*, maximum spSNA was reduced after the desipramine administration, which is consistent with previous reports observed in renal SNA (Eisenhofer et al., 1991) and cardiac SNA (Kawada et al., 2004) in rabbits. Neuronal NE uptake blockade by desipramine results in the accumulation of synaptic NE of the noradrenergic neurons in the central nervous system, which would cause presynaptic inhibition via α_2-adrenegic receptors (Svensson and Usdin, 1978). On the other hand, the accumulation of synaptic NE at the neuroeffector junction can enhance the peripheral cardiovascular response, as evidenced by the increased slope of the AP response to spSNA (Fig. 3H). The results are in agreement with enhanced NE release and AP response to spinal cord stimulation by desipramine (Yamaguchi and Kopin, 1980). Because of the enhanced peripheral cardiovascular response, maximum AP after desipramine was not much different compared with the control condition despite the lower maximum spSNA in *Protocol 2*. The enhanced peripheral cardiovascular response is, however, somewhat divergent from the effects of desipramine on dynamic baroreflex regulation, because the transfer function from cardiac SNA to AP was unchanged by desipramine (Kawada et al., 2004). While desipramine-induced accumulation of synaptic NE contributes to the maintenance of mean AP, it can reduce the relative change of synaptic NE concentration per nerve impulse, resulting in the limited dynamic AP response. As another example, desipramine decreases the dynamic gain of the hind-limb vascular conductance response to electrical stimulation of the lumber sympathetic chain (Bertram et al., 2000). These results indicate that dynamic response and steady-state response need to be separately assessed when evaluating the effects of neuronal NE uptake blockade on peripheral cardiovascular responses.

Impairment of neuronal NE uptake may contribute to the pathophysiology of sympathetic abnormality in heart failure (Backs et al., 2001) and hypertension (Rumantir et al., 2000). Cardiac overexpression of NE transporter results in functional improvement of a rabbit model of rapid pacing-induced heart failure (Münch et al., 2005). In the present study, the plasma NE concentration was significantly increased after desipramine compared with the control condition, being consistent with previous reports (Eisenhofer, 2001; Eisenhofer et al., 1991). The increase in plasma NE concentration, in conjunction with the decrease in spSNA, tripled the slope of the regression line between spSNA and plasma NE concentration (Fig. 3G). These results indicate that plasma NE concentration can be increased disproportionally to spSNA depending on the impairment of neuronal NE uptake function. While plasma NE concentration can be an index of spSNA, it could overestimate sympathetic outflow from the central nervous system under diseased conditions when they are associated with the systemic impairment of neuronal NE uptake function.

4.3. Limitations

First, data were obtained under anesthetized conditions. Because anesthesia affects the autonomic nervous activities, the present results may not be directly extrapolated to interpret sympathetic AP control under conscious conditions. Second, time resolution for plasma NE measurement was 30 s, which was by far slower than the recording of spSNA and AP. The necessity of a blood sample volume of 0.2 ml also limited the number of data points analyzed during baroreflex response compared with previous baroreflex studies (Kawada et al., 2009, 2010; Yamamoto et al., 2013). Further refinement of NE measurement to reduce sample volume and increase time resolution will be required to understand dynamic changes in plasma NE concentration during acute baroreflex control of AP.

5. Conclusion

While the logarithmic relation between plasma NE concentration and AP is commonly observed in several circumstances (Imai et al., 1994; Yamaguchi and Kopin, 1979), the relationship between spSNA and plasma NE concentration was nearly linear within the normal physiological range of the acute baroreflex control of AP. Although plasma NE concentration can be an index of spSNA, data needs to be carefully interpreted as the systemic impairment of neuronal NE uptake can increase plasma NE concentration disproportionally to sympathetic outflow from the central nervous system.

Conflict of interest statement

The authors declare that there are no conflicts of interest.

Acknowledgments

This study was supported by the Support Program to break the bottlenecks at R&D System for accelerating the practical use of Health Research Outcome from Japan Science and Technology Agency, and by the Grant-in-Aid for Scientific Research (JSPS KAKENHI Grant Number 26750153).

References

Backs, J., Haunstetter, A., Gerber, S.H., Metz, J., Borst, M.M., Strasser, R.H., Kübler, W., Haass, M., 2001. The neuronal norepinephrine transporter in experimental heart failure: evidence for a posttranscriptional downregulation. J. Mol. Cell. Cardiol. 33, 461–472.

Bertram, D., Barrés, C., Cheng, Y., Julien, C., 2000. Norepinephrine reuptake, baroreflex dynamics, and arterial pressure variability in rats. Am. J. Physiol. Regul. Integr. Comp. Physiol. 279, R1257–R1267.

DiBona, G.F., Sawin, L.L., 1999. Functional significance of the pattern of renal sympathetic nerve activation. Am. J. Physiol. 277, R346–R353.

Eisenhofer, G., 2001. The role of neuronal and extraneuronal plasma membrane transporters in the inactivation of peripheral catecholamines. Pharmacol. Ther. 91, 35–62.

Eisenhofer, G., Saigusa, T., Esler, M.D., Cox, H.S., Angus, J.A., Dorward, P.K., 1991. Central sympathoinhibition and peripheral neuronal uptake blockade after desipramine in rabbits. Am. J. Physiol. 260, R824–R832.

Glantz, S.A., 2002. Primer of Biostatistics, 5th ed. McGraw-Hill, New York.

Guyenet, P.G., 2006. The sympathetic control of blood pressure. Nat. Rev. Neurosci. 7, 335–346.

Imai, K., Higashidate, S., Prados, P.P., Santa, T., Adachi-Akahane, S., Nagao, T., 1994. Relation between blood pressure and plasma catecholamine concentration after administration of calcium antagonists to rats. Biol. Pharm. Bull. 17, 907–910.

Kahan, T., Pernow, J., Schwieler, J., Wallin, B.G., Lundberg, J.M., Hjemdahl, P., 1988. Noradrenaline release evoked by a physiological irregular sympathetic discharge pattern is modulated by prejunctional α- and β-adrenoceptors in vivo. Br. J. Pharmacol. 95, 1101–1108.

Kawada, T., Miyamoto, T., Uemura, K., Kashihara, K., Kamiya, A., Sugimachi, M., Sunagawa, K., 2004. Effects of neuronal norepinephrine uptake blockade on baroreflex neural and peripheral arc transfer characteristics. Am. J. Physiol. Regul. Integr. Comp. Physiol. 286, R1110–R1120.

Kawada, T., Kamiya, A., Li, M., Shimizu, S., Uemura, K., Yamamoto, H., Sugimachi, M., 2009. High levels of circulating angiotensin II shift the open-loop baroreflex control of splanchnic sympathetic nerve activity, heart rate and arterial pressure in anesthetized rats. J. Physiol. Sci. 59, 447–455.

Kawada, T., Li, M., Kamiya, A., Shimizu, S., Uemura, K., Yamamoto, H., Sugimachi, M., 2010. Open-loop dynamic and static characteristics of the carotid sinus baroreflex in rats with chronic heart failure after myocardial infarction. J. Physiol. Sci. 60, 283–298.

Kawada, T., Shimizu, S., Li, M., Kamiya, A., Uemura, K., Sata, Y., Yamamoto, H., Sugimachi, M., 2011. Contrasting effects of moderate vagal stimulation on heart rate and carotid sinus baroreflex-mediated sympathetic arterial pressure regulation in rats. Life Sci. 89, 498–503.

Kawada, T., Li, M., Zheng, C., Shimizu, S., Uemura, K., Turner, M.J., Yamamoto, H., Sugimachi, M., 2014. Chronic vagal nerve stimulation improves baroreflex neural arc function in heart failure rats. J. Appl. Physiol. 116, 1308–1314.

Münch, G., Rosport, K., Bültmann, A., Baumgartner, C., Li, Z., Laacke, L., Ungerer, M., 2005. Cardiac overexpression of the norepinephrine transporter uptake-1 results in marked improvement of heart failure. Circ. Res. 97, 928–936.

Nicholls, D.G., 1994. Proteins, Transmitters and Synapses. Blackwell Sciences, Oxford, UK, pp. 200–221.

Rumantir, M.S., Kaye, D.M., Jennings, G.L., Vaz, M., Hastings, J.A., Esler, M.D., 2000. Phenotypic evidence of faulty neuronal norepinephrine reuptake in essential hypertension. Hypertension 36, 824–829.

Sato, T., Kawada, T., Miyano, H., Shishido, T., Inagaki, M., Yoshimura, R., Tatewaki, T., Sugimachi, M., Alexander Jr., J., Sunagawa, K., 1999. New simple methods for isolating baroreceptor regions of carotid sinus and aortic depressor nerves in rats. Am. J. Physiol. 276, H326–H332.

Shimizu, S., Akiyama, T., Kawada, T., Shishido, T., Mizuno, M., Kamiya, A., Yamazaki, T., Sano, S., Sugimachi, M., 2010. In vivo direct monitoring of interstitial norepinephrine levels at the sinoatrial node. Auton. Neurosci. 152, 115–118.

Shoukas, A.A., Callahan, C.A., Lash, J.M., Haase, E.B., 1991. New technique to completely isolate carotid sinus baroreceptor regions in rats. Am. J. Physiol. 260, H300–H303.

Stocker, S.D., Muntzel, M.S., 2013. Recording sympathetic nerve activity chronically in rats: surgery techniques, assessment of nerve activity, and quantification. Am. J. Physiol. Heart Circ. Physiol. 305, H1407–H1416.

Svensson, T.H., Usdin, T., 1978. Feedback inhibition of brain noradrenaline neurons by tricyclic antidepressants: α-receptor mediation. Science 202, 1089–1091.

Yamaguchi, I., Kopin, I.J., 1979. Plasma catecholamine and blood pressure responses to sympathetic stimulation in pithed rats. Am. J. Physiol. 237, H305–H310.

Yamaguchi, I., Kopin, I.J., 1980. Blood pressure, plasma catecholamines, and sympathetic outflow in pithed SHR and WKY rats. Am. J. Physiol. 238, H365–H372.

Yamamoto, K., Kawada, T., Kamiya, A., Takaki, H., Sugimachi, M., Sunagawa, K., 2005. Static interaction between muscle mechanoreflex and arterial baroreflex in determining efferent sympathetic nerve activity. Am. J. Physiol. Heart Circ. Physiol. 289, H1604–H1609.

Yamamoto, H., Kawada, T., Shimizu, S., Kamiya, A., Miyazaki, S., Sugimachi, M., 2013. Effects of cilnidipine on sympathetic outflow and sympathetic arterial pressure and heart rate regulations in rats. Life Sci. 92, 1202–1207.

Heart Vessels
DOI 10.1007/s00380-014-0604-6

ORIGINAL ARTICLE

Hybrid stage I palliation for hypoplastic left heart syndrome has no advantage on ventricular energetics: a theoretical analysis

Shuji Shimizu · Toru Kawada · Dai Une · Toshiaki Shishido · Atsunori Kamiya · Shunji Sano · Masaru Sugimachi

Received: 26 May 2014 / Accepted: 14 November 2014

Abstract A hybrid procedure combining bilateral pulmonary artery banding with ductal stenting has recently been used as stage I palliation for hypoplastic left heart syndrome. However, the advantage of the hybrid procedure over the Norwood procedure on ventricular energetics remains unclear. To clarify this, we performed a computational analysis with a combination of time-varying elastance chamber model and modified three-element Windkessel vascular model. Although mean pulmonary artery (PA) pressure, pulmonary flow, and oxygen saturation were almost equivalent with the Norwood procedure, the hybrid procedure delivered higher systolic and lower diastolic systemic arterial pressures compared to the Norwood procedure with right ventricle (RV) to PA shunt. As a result, the hybrid procedure yielded increased systolic pressure–volume area and impaired mechanical efficiency. Therefore, the hybrid procedure has probably no advantage on ventricular energetics compared to the Norwood procedure with a RV-PA shunt.

Keywords Hypoplastic left heart syndrome · Hybrid procedure · Norwood procedure · Ventricular energetics · Computational model

S. Shimizu (✉) · T. Kawada · D. Une · T. Shishido · A. Kamiya · M. Sugimachi
Department of Cardiovascular Dynamics, National Cerebral and Cardiovascular Center, 5-7-1 Fujishiro-dai, Suita, Osaka 565-8565, Japan
e-mail: shujismz@ri.ncvc.go.jp

S. Shimizu · S. Sano
Department of Cardiovascular Surgery, Okayama University Graduate School of Medicine, Dentistry and Pharmaceutical Sciences, 2-5-1 Shikata-cho, Kita-ku, Okayama, Okayama 700-8558, Japan

Introduction

Advances in surgical techniques for hypoplastic left heart syndrome (HLHS) in the past several decades have improved outcomes after stage I palliation. In 1993, Gibbs et al. [1] first reported stenting of the arterial duct combined with banding of the pulmonary arteries and atrial septectomy or septostomy as a new palliation approach for HLHS. Since this approach can be performed without the use of cardiopulmonary bypass (CPB), the hybrid procedure has recently been conducted as stage I palliation for HLHS to salvage high-risk neonates [2]. Several studies demonstrated its comparable outcomes to those of the Norwood procedure [3, 4]. At the same time, despite the lower invasiveness, a recent study reports that this procedure does not improve outcome with respect to survival beyond stage II palliation [5] compared to the Norwood procedure. Furthermore, Sasaki et al. [6] reported that this procedure was associated with high interstage morbidity.

On the other hand, since Sano et al. [7] reported their experience with the right ventricle (RV)-to-pulmonary artery (PA) shunt as a modification of the Norwood procedure in 2003, this modified procedure has been performed widely with lower interstage mortality [8]. The reason why this modification improves interstage mortality may be due to the improvement of ventricular energetics. Lee et al. [9] have reported that RV stroke work (SW) may be useful to quantify RV inefficiency. Bove et al. [10] have reported that the RV-PA shunt demonstrates lower SW and higher mechanical efficiency. We have also reported that the RV-PA shunt reduces systolic pressure–volume area (PVA) and increases mechanical efficiency in spite of the presence of diastolic regurgitation [11].

The reason why the hybrid procedure does not improve outcome despite its less invasiveness may be that the

Published online: 29 November 2014

hybrid procedure probably impairs ventricular energetics compared to the Norwood procedure. However, it is very difficult to compare ventricular energetics among the different surgical procedures in the clinical settings because postoperative hemodynamic profiles, even heart rate and mean arterial pressure, are quite different among the palliations [12]. The lack of proper methodology to accurately measure hemodynamic parameters such as stroke volume in congenital heart diseases also limits the study in clinical settings. Therefore, to test the hypothesis that ventricular energetics are different among the palliations, we performed a theoretical analysis using computational models.

Materials and methods

We modeled the cardiovascular system for the hybrid procedure and that for the Norwood procedure using a systemic-to-pulmonary artery (SPA) shunt or a RV-PA shunt. The electrical analog of the hybrid procedure model used to simulate the cardiovascular system is shown in Fig. 1. Details of the Norwood procedure models with a SPA shunt and with a RV-PA shunt have been described previously [11]. Aortic and mitral atresias were assumed in all of the present models, and there was no left ventricle.

Heart

The ventricular and atrial chambers are represented by the time-varying elastance model [11, 13–15]. Pressure and volume of each chamber are related by

$$P_{cc}(t) = \left[P_{es,cc}(V_{cc}) - P_{ed,cc}(V_{cc})\right] e_{cc}(t) + P_{ed,cc}(V_{cc}) \quad (1)$$

$$P_{ed,cc} = A_{cc}\left[e^{B_{cc}(V_{ed,cc}-V_{0,cc})} - 1\right] \quad (2)$$

$$P_{es,cc} = E_{es,cc}[V_{es,cc} - V_{0,cc}] \quad (3)$$

$$e_{cc}(t) = 0.5[1 - \cos(\pi t/T_{es,cc})] \quad (0 \le t < 2T_{es,cc})$$

$$e_{cc}(t) = 0 \quad (2T_{es,cc} \le t < T_c), \quad (4)$$

where P_{cc} and V_{cc} are pressure and volume, respectively, of each chamber [cc denotes the right atrial (RA), left atrial (LA), or right ventricular (RV) chamber], and t is the time from the start of systole. We modeled chamber pressure as the sum of end-diastolic pressure ($P_{ed,\,cc}$, Eq. 2) and the developed pressure [difference between end-systolic ($P_{es,\,cc}$, Eq. 3) and $P_{ed,\,cc}$] scaled by normalized elastance [$e_{cc}(t)$, Eq. 4]. Other parameters are listed in Table 1 [11, 13–16]. The time advance of atrial systole (DT) is calculated as $DT = 0.02T_c$ [11, 16].

Restrictive atrial septal defect (R_{ASD}) is described as a constant resistance, and the value in the hybrid procedure model was set 10 times higher than those of the Norwood procedure models. Each valve is represented as an ideal diode connected serially to a small resistor (pulmonary, R_{PV}; tricuspid, R_{TV}).

Vascular system

Pulmonary and systemic circulations are modeled as modified Windkessel models. Each vasculature is modeled by lumped venous (C_v) and arterial (C_a) capacitances, a characteristic impedance (R_c), arterial resistance (R_a), and a resistance proximal to C_v (R_v). Linear relation between pressure drop and flow in each resistance (except for PA banding), relation

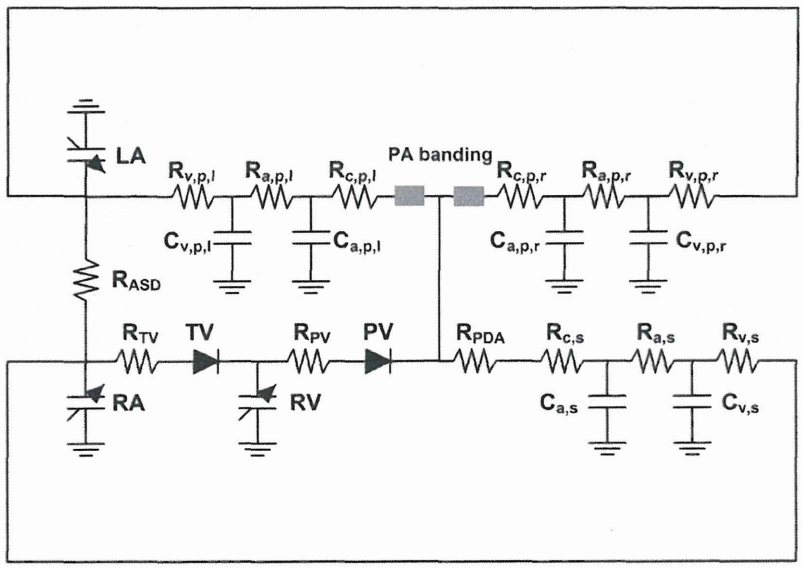

Fig. 1 Electrical analog of the hybrid procedure. *LA* left atrium, *RA* right atrium, *RV* right ventricle, *PV* pulmonary valve, *TV* tricuspid valve, *ASD* atrial septal defect, *PDA* patent ductus arteriosus, R_a arterial resistance, R_c characteristic impedance, R_v venous resistance, C_a arterial capacitance, C_v venous capacitance. *s* and *p* denote systemic and pulmonary circulation, respectively. *l* and *r* denote *left* and *right* sides, respectively. R_{PV}, R_{TV}, R_{ASD} and R_{PDA} represent resistance at PV, TV, ASD and PDA, respectively

Table 1 Parameters used in modeling of hybrid procedure

Heart rate (HR) (beats/min)			150
Duration of cardiac cycle (T_c) (ms)			400
	RV	RA	LA
Time to end systole (T_{es}) (ms)	140	60	60
End-systolic elastance (E_{es}) (mmHg/ml)	8.5	7.35	7.35
Scaling factor of EDPVR (A) (mmHg)	0.9	0.17	0.17
Exponent for EDPVR (B) (ml^{-1})	0.062	0.484	0.484
Unstressed volume (V_0) (ml)	4	1	1
	Pulmonary		Tricuspid
Valvular resistance (forward) (mmHg s ml^{-1})	0.0004		0.00004
Resistance (mmHg s ml^{-1})	ASD		
	0.01		
Resistance (mmHg s ml^{-1})	PDA		
	0.0004		
	PA banding		
Diameter of proximal PA (D_{PA}) (mm)	5.0		
Constant (k) (mmHg $(l/s)^{-2}$ mm^4)	1.62×10^6		
	Systemic (s)	Pulmonary (p)	
		Lt. (l)	Rt. (r)
Arterial resistance (R_a) (mmHg s ml^{-1})	3.83	1.56	1.04
Characteristic impedance (R_c) (mmHg s ml^{-1})	0.20	0.071	0.047
Venous resistance (R_v) (mmHg s ml^{-1})	0.083	0.027	0.018
Arterial capacitance (C_a) (ml/mmHg)	0.50	0.13	0.19
Venous capacitance (C_v) (ml/mmHg)	4.39	0.36	0.53

RV right ventricle, *RA* right atrium, *LA* left atrium, *EDPVR* end-diastolic pressure–volume relation, *ASD* atrial septal defect, *PDA* patent ductus arteriosus, *PA* pulmonary artery, *Lt* left, *Rt* right

between pressure (P_c) and volume (V_c) in each capacitance C (Eq. 5), and the change in volume in each capacitance [$dV(t)/dt$] calculated by the difference between inflow and outflow (Eq. 6) are used to describe each vasculature:

$$P_c = \frac{V_c}{C} \tag{5}$$

$$\frac{dV(t)}{dt} = \sum Q_{inflow}(t) - \sum Q_{outflow}(t) \tag{6}$$

where $Q_{inflow}(t)$ and $Q_{outflow}$ (t) are volumetric inflow and outflow, respectively.

Ideal ductal stenting without stenosis (R_{PDA}) is described as a constant resistance.

Pressure drop across the PA banding

Combining the Bernoulli's principle, the relation between PA flow velocity V (V_{PAB}, banding site; V_{PA}, PA proximal to the banding site), volumetric flow of the right or left PA $Q(t)$, and PA diameter D (D_{PAB}, banding site; D_{PA}, proximal PA) are represented as follows:

$$\Delta P(t) = \frac{1}{2}\rho\left(V_{PAB}^2 - V_{PA}^2\right), \quad V_{PAB} = \frac{4Q(t)}{\pi D_{PAB}^2}, \quad V_{PA} = \frac{4Q(t)}{\pi D_{PA}^2}$$

And, pressure drop across the PA banding [$\Delta P(t)$] is described as

$$\Delta P(t) = k\left(\frac{1}{D_{PAB}^4} - \frac{1}{D_{PA}^4}\right)Q(t)^2, \quad k = \frac{8\rho}{\pi^2}, \tag{7}$$

where ρ is blood density ($\rho = 1.06$ g/cm^3), and k is constant if the blood density does not change.

Protocols

First, the control state was simulated using the 4.0-mm SPA shunt Norwood procedure model. Total stressed blood volume (V_s), which is the sum of the stressed volumes in all capacitances and in all chambers, was set as 81.4 ml.